Physica B 151 (1988) 262–272
North-Holland, Amsterdam

ULTRA-HIGH SENSITIVITY ACCELEROMETERS AND GYROSCOPES USING NEUTRAL ATOM MATTER-WAVE INTERFEROMETRY*

John F. CLAUSER
975 Murrieta Boulevard 22, Livermore, CA 94550, USA

This paper shows that matter-wave interferometers employing low-velocity neutral atoms can be used as inertial sensors with sensitivities that exceed those of conventional mechanical sensors and multiple circuit optical interferometers by many powers of ten. The energy and mass dependence of the phase shifts that are due to rotation and acceleration are different. Thus a pair of interferometers with different energies and/or masses can perform simultaneous independent measurements of rotation and acceleration. A proposed configuration is one formed by a sequence of planar diffraction gratings operating in high order. Gratings consist of near-resonant standing-wave laser beams. Laser decelerated and cooled atomic beams provide a suitable source. Path curvature due to acceleration and rotation is canceled by magnetic field gradients that produce an effective magnetic levitation of the atoms in a feedback arrangement that maintains null phase shift.

1. Introduction

Inertial sensors are useful devices in both science and industry. Scientific applications abound in the areas of general relativity, geodesy and geology. Important practical applications of such devices occur in the fields of navigation, surveying and the analysis of structures. This paper will show that the use of separated-beam neutral atom matter-wave interferometers as inertial sensors can improve the attainable sensitivities for such sensors by many powers of ten over the current state of the art. Additionally, these interferometers are highly sensitive spectrometers in their own right and have other uses. Perturbations of an atom's total energy on the order of Planck's constant per second are readily measurable. Further scientific applications then include measurements of the so-called composition dependent fifth force, symmetry violating effects in atomic systems, etc. Indeed, virtually all of the elegant experiments within the reach of an atomic beams machine can be performed with such a device, as well as many more for measurements of effects that do not result in a shift of an atom's Zeeman level splitting**.

Even a casual observation of the capabilities of a matter-wave interferometer will convince the reader that its gyroscopic sensitivity is inherently high. With such a system employing neutrons, phase shifts due to rotation (the analog of the Sagnac effect [1]) have been observed by Werner, Staudenmann and Colella [2] and those due to gravity by Colella, Overhauser and Werner [3]. The experiment by Werner et al. measured the rotation rate of the earth with an interferometer whose area was but a few square centimeters. In contrast, the classic experiment by Michelson and Gale [4] required an area many times that of a soccer field to accomplish the same measurement with an optical interferometer. When the mass and energy scalings of the phase shift of a matter-wave interferometer are exploited, the sensitivity can become dazzlingly high. Excellent reviews of the neutron ex-

* Work supported personally and solely by the author. Patent applied for.

** In an atomic beams machine, interference occurs between propagations along the same path but in different angular momentum states. In a separated beam interferometer, interaction with an atom can occur independently of its angular momentum, and the interaction can be applied locally to only one beam.

periments have been given by Werner [5], Klein and Werner [6] and by Greenberger and Overhauser [7].

2. Sensitivity of matter-wave interferometers to inertial forces

How does one sense inertial forces? Departures from an inertial reference frame are limited by Euler's and Chasle's theorems of classical mechanics to rotations and translations. Relativity and the equivalence principle further limit locally observable fictitious forces to those due to rotation and acceleration plus gravity. These forces can be sensed by gyroscopes and accelerometer/gravimeters. A two-separated-beam interferometer employing either electromagnetic waves or matter waves is also sensitive to such forces. Its sensitivity, however, strongly depends upon the type of waves that propagate within it.

Consider a symmetric two-separated-beam interferometer with a geometry similar to that of Young's two-slit experiment. The geometry is shown in fig. 1, with the double slit midway between the source and detector. Suppose this interferometer is used with matter waves associated with particles of mass m. The flux of particles impinging on the screen at various locations will form an interference pattern that can be measured. Let x be the distance between the source slit and the detector, and let y be half the double-slit spacing. Additionally, let $\hat{o}$ be a unit vector perpendicular to the plane of the paths, let A be the enclosed area xy, let $\hat{q}$ be a unit vector perpendicular to the line between the source and detector, and let L be the slant distance from the source slit to either of the detector slits, i.e. $L = (x^2/4 + y^2)^{1/2}$.

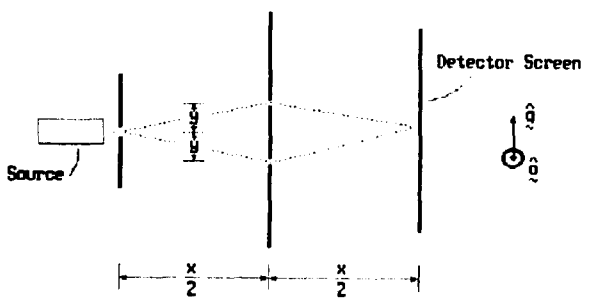

Fig. 1. Geometry of Young's two-slit experiment.

If the interferometer is not located in an inertial reference frame, there will be a resulting phase shift. One may consider the matter waves as propagating in a non-inertial reference frame and calculate the phase shift by evaluating the effects of the Coriolis, centrifugal and gravitational potentials. Let $\boldsymbol{\Omega}$ be the rotation rate vector, and $\boldsymbol{g}$ be the sum of the acceleration and gravity vectors. Also, assume that a magnetic field $\boldsymbol{B}$ is present, and that the particles each have a magnetic moment $\boldsymbol{\mu}$, everywhere parallel to $\boldsymbol{B}$. Further, assume that the gradients of $\boldsymbol{B}$ are sufficiently small that their probability of inducing a spin flip (Majoranna transition) is negligible [8]. Then the Hamiltonian for the particles is given by [9]

$$\mathcal{H} = \frac{1}{2m}(\boldsymbol{p} - m\boldsymbol{\Omega} \times \boldsymbol{r})^2 - \frac{m}{2}(\boldsymbol{\Omega} \times \boldsymbol{r})^2 + m\boldsymbol{g} \cdot \boldsymbol{r} - \boldsymbol{\mu} \cdot \boldsymbol{B}(\boldsymbol{r}),$$

where the various terms represent the kinetic energy with the Coriolis potential included as part of the canonical momentum, the centrifugal potential, the gravitational potential, and the Zeeman potential, respectively. Here, $\boldsymbol{p}$ is the particle's momentum operator, and $\boldsymbol{r}$ is the particle's position operator referenced from the axis of rotation. Since the operator $\boldsymbol{\Omega} \times \boldsymbol{r}$ is orthogonal to $\boldsymbol{r}$, it commutes with $\boldsymbol{r}$, and we can write

$$\mathcal{H} = \frac{\boldsymbol{p}^2}{2m} - \boldsymbol{\Omega} \times \boldsymbol{r} \cdot \boldsymbol{p} + m\boldsymbol{g} \cdot \boldsymbol{r} - \boldsymbol{\mu} \cdot \boldsymbol{B}(\boldsymbol{r}).$$

The solution to the Schrödinger equation, $\mathcal{H}\psi = E\psi$, for the phase of ψ at the detector is simplified by the use of the WKB approximation. To implement this, we take the paths to be composed of piece-wise linear segments. Along a segment we represent the unit vector parallel to it by the symbol $\hat{t}$, and the distance along it by the scalar function $s(\boldsymbol{r})$. We then search for a function $u(s)$ so that we can represent ψ in the form $\psi = \exp[\mathrm{i}\, u(s)]$. Applying the WKB approx-

imation, we neglect the term d^2u/ds^2 relative to the term $(du/ds)^2$. For propagation of matter waves along a path from points a to b, we have the phase at b relative to that at a given by the line integral.

$$u = \int_a^b \left\{ -\frac{m\boldsymbol{\Omega} \times \boldsymbol{r}(s) \cdot \hat{\boldsymbol{t}}}{\hbar} + \left[\left(\frac{m\boldsymbol{\Omega} \times \boldsymbol{r}(s) \cdot \hat{\boldsymbol{t}}}{\hbar} \right)^2 - \frac{2m}{\hbar^2} [m\boldsymbol{g} \cdot \boldsymbol{r}(s) - \boldsymbol{\mu} \cdot \boldsymbol{B}(s) - E] \right]^{1/2} \right\} ds ,$$

where $h = 2\pi\hbar$ is the Planck constant. Here, we have taken the + sign in front of the radical corresponding to waves that propagate in the $+s$ direction. The phase difference along two such paths is then the difference between the integrals along these paths. The above expression can be simplified when the kinetic energy $p^2/2m$ is large with respect to the various potential energies, whereupon we can approximate the phase difference at b as

$$\delta u = -\frac{2mA}{\hbar} \boldsymbol{\Omega} \cdot \hat{\boldsymbol{o}} - \frac{m^{3/2}}{\hbar E^{1/2} 2^{1/2}} \oint [\boldsymbol{g} \cdot \boldsymbol{r}(s)] \, ds + \frac{m^{1/2}}{\hbar E^{1/2} 2^{1/2}} \oint [\boldsymbol{\mu} \cdot \boldsymbol{B}(s)] \, ds + \frac{m^{3/2}}{\hbar E^{1/2} 2^{3/2}} \oint [\boldsymbol{\Omega} \cdot \boldsymbol{r}(s) \times \hat{\boldsymbol{t}}]^2 \, ds .$$

The first term was further simplified via Stoke's theorem. The last term represents the contribution due to centrifugal force. It has been neglected by previous workers. It may be incorporated into the gravitational acceleration when the radius, $\boldsymbol{r}$, is large with respect to the dimensions of the interferometer, and gives significant contribution only at large $\boldsymbol{\Omega}$.

To explore the possibilities for use of such an interferometer as an inertial sensor, let us compare its sensitivity to rotation and acceleration with that of an optical interferometer with the same rhombus geometry indicated above. Keeping only the Coriolis and linear acceleration terms, we have approximately for the phase shift, that is due to rotation,

$$\delta_{\text{gyro}}(m > 0) = \frac{4\pi m A(\boldsymbol{\Omega} \cdot \hat{\boldsymbol{o}})}{h} ,$$

for a matter-wave interferometer, while for an optical interferometer the analogous phase shift is

$$\delta_{\text{gyro}}(\text{light}) = \frac{4\pi A(\boldsymbol{\Omega} \cdot \hat{\boldsymbol{o}})}{\lambda c} ,$$

where λ is the wavelength of the light and c is the speed of light. Correspondingly, for linear acceleration, we have the phase shift for a matter-wave interferometer,

$$\delta_{\text{accel}}(m > 0) = \frac{m^{3/2} 2^{1/2} L y (\boldsymbol{g} \cdot \hat{\boldsymbol{q}})}{\hbar E^{1/2}} ,$$

while the analogous phase shift for an optical interferometer is

$$\delta_{\text{accel}}(\text{light}) = \frac{4\pi L y (\boldsymbol{g} \cdot \hat{\boldsymbol{q}})}{\lambda c^2} .$$

The ratio of the gyroscopic sensitivities is

$$R_{\text{gyro}} = m\lambda c h^{-1} ,$$

while the ratio of the accelerational sensitivities is

$$R_{\text{accel}} = 2m\lambda c^2 v^{-1} h^{-1} ,$$

where v is the particle velocity.

The scalings indicate that for a given area, high-mass low-velocity particles will produce the best sensitivity. Suppose one uses particles many times heavier than a neutron. Recent experiments on laser deceleration and cooling of atomic beams [10] can readily produce nearly mono-energetic neutral sodium beams with a velocity of $50\ \text{m s}^{-1}$ and much slower*. Contrast

* Diminishing energy resolution and density occurs at low velocity in the continuous technique by Prodan et al. [10] as a result of difficulties in extracting slow atoms from a magnetic field in the presence of the laser beam. Alternative magnetic field configurations and/or maintaining the interferometer in the same field will allow production of much slower beams.

a matter-wave interferometer employing such a beam with an optical interferometer at $\lambda = 5000$ Å. The matter-wave interferometer is more sensitive to rotation by a factor $R_{gyro} \approx 10^{10}$, and to acceleration by a factor $R_{accel} \approx 10^{17}$. Presumably a heavy atom such as mercury can be decelerated to a velocity slower by at least the square root of the mass ratio i.e. 17 m/s. Then these ratios become $R_{gyro} \approx 10^{11}$ and $R_{accel} \approx 3 \times 10^{18}$, respectively. In a configuration discussed below, the interferometer produces its own velocity selection so that residual velocity spread is not problematic.

The gyroscopic and accelerational sensitivities of a matter-wave interferometer, unlike an optical interferometer*, depend differently on particle mass and energy. Thus a pair of matter-wave interferometers employing different masses and/or energies can be used to determine both acceleration and rotation rate simultaneously from a solution of the simultaneous equations. An instrument comprised of six interferometers, each sensing a different component of $\boldsymbol{\Omega}$ and $\boldsymbol{g}$, can thus be employed to measure simultaneously all three components of each of $\boldsymbol{\Omega}$ and $\boldsymbol{g}$.

The sensitivities of both matter-wave and optical interferometers can be increased by allowing multiple circuits about the enclosed area, and by increasing the enclosed area. Although an extremely large number of circuits can easily be accomplished in an optical interferometer (i.e. in a ring laser) the present state of the art at doing so without introducing a large number of new deleterious effects limits optical interferometers to sensitivity values well below those expected for matter-wave interferometers [11].

3. A configuration for a neutral atom interferometer

A neutral-atom separated-beam interferometer has not yet been built [12]. Many configurations are conceivable. In this paper we discuss a configuration that capitalizes on two recent advances in atomic beam technology. The first is the aforementioned advance in the art for producing slow cool atomic beams. The second is the demonstration by Gould, Ruff and Pritchard [13] for producing a planar diffraction grating for neutral sodium atoms in the form of a standing-wave laser beam that is nearly resonant with an atomic resonance transition. In their experiment, significant usable intensity is produced in eighth- and higher-order diffraction with the various orders cleanly resolved.

Diffraction grating interferometers have been built for light [14], electrons [15], and neutrons [16]. Such interferometers can be configured in a variety of ways in both laterally symmetric and asymmetric configurations. Some of these are shown in fig. 2. The use of Bragg diffraction in electron and neutron matter-wave interferometry limits the selection of diffraction orders usable in a grating interferometer. The limitation does not apply to interferometers that use planar (two dimensional) gratings. Thus, all of the configurations shown can operate in high order. Greater deflection angles can be achieved with increased grating laser power, or by stacking a sequence of planar gratings.

The chromatic properties of an interferometer formed from a sequence of gratings are quite remarkable. Laterally symmetric cases provide a natural focusing mechanism for the paths onto the superposition region that is independent of the wavelength. Focusing is useful to provide a high throughput flux when the input atomic beam contains a wide spread of wavelengths. All cases provide a dispersive mechanism that facilitates selection of a narrow band of wavelengths from among those in the input beam. Thus, if collimation limits the incidence on the gratings, then the gratings will act as velocity selectors, so that the source need not be monochromatic (except as is needed to prevent overlapping orders and provide high source intensity).

Consider a symmetric neutral atom interferometer with the geometry shown in fig. 2b, comprised of a sequence of three near-resonant standing-wave laser beams acting as diffraction gratings. Atoms impinging from the left are diffracted into orders $\pm n$ at angles

* Of course, a distinction between rotation and acceleration can be made by an optical interferometer through the different geometric dependencies on these.

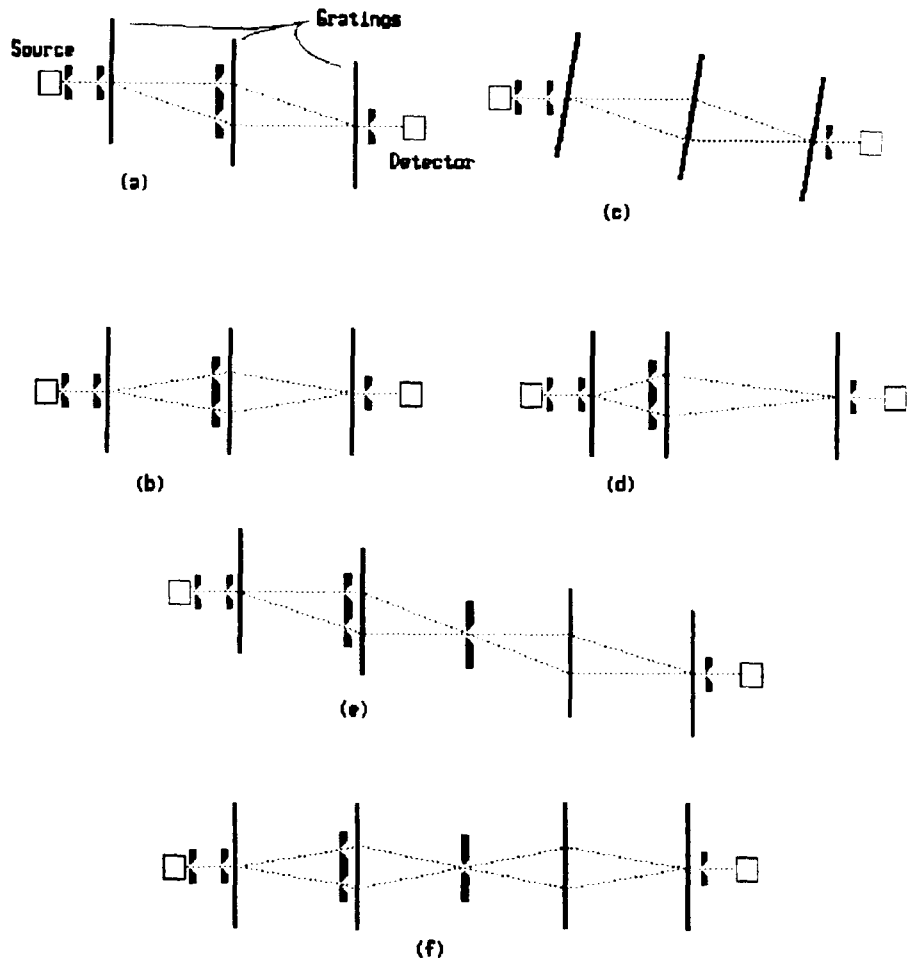

Fig. 2. (a) Geometry of a simple laterally asymmetric longitudinally symmetric grating interferometer. This configuration was employed by Marton et al. [15] as an electron interferometer. (b) Geometry of a simple laterally and longitudinally symmetric grating interferometer. (c) Modification of (a) with tilted gratings. This configuration was employed by Bonse and Hart [16] for a neutron interferometer. (d) Geometry of a simple laterally symmetric but longitudinally asymmetric grating interferometer. (e) Geometry of a figure-eight path laterally asymmetric grating interferometer. (f) Geometry of a figure-eight path laterally symmetric grating interferometer. Configurations (e) and (f) have zero sensing area and are useful for measuring gravitational gradients.

$\theta = \pm 2n\lambda_{\text{atom}}/\lambda_{\text{laser}}$.

Diffraction at the middle grating is then in orders $\pm 2n$. For an overall interferometer length x, the enclosed area is given by $A = \theta x^2/2$. For such a system, the phase shift due to rotation is given by

$$\left[\frac{\delta}{\pi}\right]_{\text{gyro}} \approx \frac{4x^2 n(\boldsymbol{\Omega}\cdot\hat{\boldsymbol{o}})}{\lambda_{\text{laser}} v_{\text{atom}}} ,$$

while that due to acceleration plus gravity is given by

$$\left[\frac{\delta}{\pi}\right]_{\text{accel}} \approx \frac{2x^2 n(\boldsymbol{g}\cdot\hat{\boldsymbol{q}})}{\lambda_{\text{laser}} v_{\text{atom}}^2} .$$

Notice that the dependence on particle mass has disappeared (except in its influence on the production of slow atoms) because of its effect on the de Broglie wavelength. Compared to a

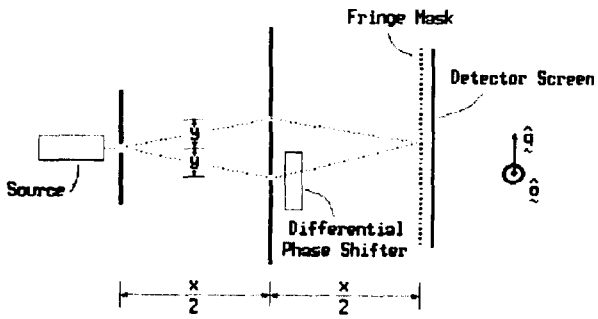

Fig. 3. Geometry of fig. 1, modified to include a fringe mask, differential phase shifter and a single detector.

square optical interferometer that uses the same wavelength light as λ_{laser}, with the same diagonal length x, the neutral atom interferometer's sensitivity to rotations is higher by a factor c/v_{atom}, and to accelerations by a factor c^2/v_{atom}^2, even though it uses a trivial fraction of the square area.

4. Interferometer parameters

Is it possible to define a realistic set of parameters for a neutral atom interferometer? For demonstration purposes, we shall confine our discussion to highly conservative estimates. Since the parameters for generating slow sodium beams are best known, we shall employ a continuous sodium beam at 50 m/s with a velocity spread about 10 m/s. The de Broglie wavelength of the atoms is 3.4 Å. (The interferometer sensitivity is mass independent, and mass now only affects how slow the atomic beam will be.) If the whole interferometer is maintained at a magnetic field comparable to that at the end of the tapered field, production of a beam with even lower velocity is now straightforward [17].

Consider a symmetric interferometer with $n = \pm 10$ at the first grating and $n = \pm 20$ at the middle gratings. The grating transmission for order n is given by $|J_n(\xi)|^2$, where ξ is proportional to laser power and inversely proportional to laser detuning. By "blazing" the gratings to maximize transmission, one then expects throughputs of 0.09 and 0.06 into respective orders 10 and 20. (Most of the wasted transmission will be either in a few adjacent orders or at least 10 orders away.) The deflection angle into $n = 10$ for a laser at 5892 Å will be 1.15×10^{-2} rad. For an overall interferometer length $x = 5$ m, the beam displacement will be $y = 2.9$ cm with an order spacing of 2.9 mm. Suppose we collimate the beam at the first and second gratings by 1 cm long slits with widths 25 μm and 125 μm respectively, yielding about 0.5% velocity spread at the second grating. If the parallel and perpendicular velocity spreads (following cooling) are comparable to each other, then about 5% of the beam will be in the desired velocity interval.

Self-scattering of the beam will limit the allowable density in the vicinity of the first grating. Assume an allowable mean free path, at low velocity, of say 20 cm (greater than the propagation from the cooling region to the first grating, and greater than the distance necessary for the various diffraction orders to separate). For a resonant cross-section [18] of 10^4 Å^2 we find a density limit here of 4×10^{10} cm^{-3}, with a corresponding limit of 5×10^{11} atoms/s passing through the first slit. This is two orders of magnitude less than the number that can be cooled by a 1 W laser, and two orders of magnitude less than what can be produced by a self-scattering limited oven with 25 μm slits 1 m away [19]. Thus, with the above grating and velocity selection efficiencies, we should be able to achieve a detector current of $\approx 10^8$ atom/s.

The necessary conditions for obtaining acceptable fringe visibility have been discussed by Chang et al. [20] for light, but their results are equally applicable to a matter-wave interferometer. The necessary coherence condition is

$$\Delta\theta \, n \, \Delta z \, 2/\lambda_{laser} \ll 1 ,$$

where $\Delta\theta$ is the collimation divergence and Δz is the grating thickness (and longitudinal thickness of the interference region). For the above parameters the grating thickness is thus limited to less than 0.6 mm.

Thus, even with our extremely conservative velocity estimates, the sensitivity of the interferometer to acceleration will be 3×10^{-4} cm/s^{-2} (=0.3 μg) per fringe, while that due to rotation will be 3×10^{-8} rad/s (=6×10^{-3} deg/h) per fringe. Depending upon the counting statistics and integration time, small fractions of a single fringe can be detected. Thus, the gyroscopic stability at the above count rate (if limited by counting statistics alone) will be about 10^{-8} deg/h$^{1/2}$.

Greater sensitivities are readily possible with larger systems, shorter λ_{laser}, higher-order diffraction, diffraction by crystal surfaces (see below) and/or slower atoms. If achievably low velocities scale inversely with the square root of the mass, employing Cs^{133} at 17 m/s (with $\lambda_{laser} = 4555$ Å) achieves a sensitivity to accelerations of 18 ng per fringe. Current state of the art gyro sensitivity is not much better than 0.001°/h, while that of accelerometers is not much better than 1 μg. The quantum noise limited stability of a 35 μW dithered active laser gyro [11] is about 10^{-3} deg/h$^{1/2}$. It is noteworthy that the Lense–Thirring and de Sitter precession rates are of order 1.5×10^{-9} deg/h and appear within the sensitivity limits of an experiment with an integration time of a few days (and/or larger enclosed area and slit dimensions). For comparison with the above accelerometer sensitivity, the effect of the sun and moon on local gravity is of the order 0.1 μg. A 10^3 kg mass at a distance of 1 m will provide a force comparable to that of 7 ng, while the composition dependent force has an expected magnitude of 10 ng.

5. Limiting beam sag

The above phase-shift calculations have neglected transverse displacements of the paths that are due to the effects of rotation and acceleration, and have assumed straight-line trajectories. In the presence of rotational and gravitational forces, a beam will be deflected and will exhibit the curved trajectory of a classical particle. The curvature will increase with increasing rotation rate and/or acceleration. At even moderate values of these, the curvature may be large enough to prevent the beam from reaching the detector(s). As a result, it is imperative that this curvature be removed for the operation of a matter-wave interferometer as an inertial sensor system with even modest dynamic range.

Additional potentials can be applied along the particle propagation paths to remove most or all of this curvature. That is, in order to maintain straight beam propagation paths, one can apply an external compensating force to the atoms that cancels the deflecting inertial forces. Such a force is available via the magnetic field that was included in the above Hamiltonian, which can be rewritten in the form

$$\mathcal{H} = \frac{p^2}{2m} + \boldsymbol{r} \cdot (\boldsymbol{\Omega} \times \boldsymbol{p} + m\boldsymbol{g} - \boldsymbol{\mu}_z \nabla \boldsymbol{B}_z) ,$$

for $\boldsymbol{B} \| \boldsymbol{\mu} \| \hat{\boldsymbol{e}}_z$. If the magnetic field gradient, $\nabla \boldsymbol{B}_z$, is selected to make the vector factor in parentheses vanish, then the Hamiltonian will be that of a force free particle with a straight trajectory. We note that the chosen interferometer geometry is symmetrical and highly elongated, with all momenta in approximately the same direction. Suppose one applies a magnetic field gradient

$$\nabla \boldsymbol{B}_z = [\boldsymbol{\Omega} \times (\boldsymbol{p}_u + \boldsymbol{p}_\ell)/2 + m\boldsymbol{g}]/\boldsymbol{\mu}_z ,$$

where $(\boldsymbol{p}_u + \boldsymbol{p}_\ell)/2$ is the average of the atomic momentum along the upper and lower paths, i.e. the average momentum along the axis. This field exactly cancels the accelerational potential and gives equal (but very small) contributions to the Hamiltonian from the Coriolis potential for the upper and lower paths. Not only does it straighten the propagation paths, it also eliminates the interferometer phase shift. Thus one can build a feedback system that maintains an interferometer phase null, and deduce the inertial effects from its error signal. For an interferometer geometry lacking the above symmetry, and/or one which must operate in a high rotation rate environment, mounting the system on servo controlled gimbals provides an alternative means for compensating the Coriolis potential. For typical atoms, gradients of a few hundred gauss per centimeter are sufficient to magnetically levitate atoms in a 1 g gravitational field. In systems using polar molecules in place of atoms, electric

field gradients will accomplish the same end as do the magnetic fields discussed here.

6. Differential phase shifter

Consider an alternative configuration to that of fig. 1, shown in fig. 3. An adjustable phase shifter has been inserted in one of the matter-wave paths. A fringe mask covers a single detector. The fringe mask consists of a set of slits, parallel to the interferometer slits. The maxima and minima of the fringes essentially form a transverse standing matter wave across the mask. Suppose that we specify that the slit spacing is equal to the transverse spacing of the matter-wave fringes, and that the mask is transversely positioned so that all bright fringes align with the slits in the mask for some value of inserted phase delay. Then for that value of delay the beam will pass through the mask to the detector. As a function of inserted delay there will be a sinusoidal variation of the detected flux. The interferometer phase shift can be detected by measuring the phase of this variation. Contributions from different velocities (e.g. those due to overlapping diffraction orders) will produce different frequency variations and can be readily measured. From considerations of the above Hamiltonian, one can see that a uniform (gradient-free) magnetic field applied to either path will provide a phase shifter that does not deflect the propagation paths.

7. Fringe magnifier and detector

The last grating of a grating interferometer essentially forms the fringe mask discussed above. Suppose that this grating is configured so that its effective slit spacing is slightly different from that of the transverse standing matter-wave. Its transmission will evidence a slow transverse periodic variation. That is, a Moiré pattern is formed. The resulting transmission variation will then form a highly magnified matter-wave interference fringe pattern.

In the presence of a standing-wave laser grating, depending upon the extent of its detuning, the atoms will fluoresce. Such a grating thus also forms a spatially periodic fluorescent screen. Light emitted by this screen can be imaged by an optical system and used to detect the fringes. If the grating wavelength is slightly different from that of the previous gratings, or more easily, if the last grating has the same wavelength of the previous gratings but is tilted slightly so as to give it the effect of a slightly different wavelength, then the result will be a magnified fringe pattern, formed by the fluorescence intensity emitted by the screen. This variation can be imaged or further magnified by the optical system and provides a very convenient fringe magnifier and detector.

8. Measuring gravitational gradients

Gravitational gradients can be measured by the apparatus described above by simply building two interferometers and displacing them from each other in position. However, a simpler and more accurate system utilizing the same principles can be built. Interferometer geometries in which the two paths follow a two loop (figure-eight) structure are shown in figs. 2e and 2f. The two loops are configured to have equal areas. Because the circuits about the two loops are oppositely directed, the net area that the matter waves circuit is zero. As a result, the interferometer will be insensitive to rotation, at least to the extent that one can neglect centrifugal acceleration. If the gravitational field acting on one of the loops is slightly different from that acting on the other loop, then the phase shifts due to gravity in the two loops will not exactly cancel each other, but will result in a net phase shift that is proportional to this difference. Thus, an interferometer with such a geometry will measure gravitational gradients. It will also measure accelerational gradients such as those due to centrifugal force. An orthogonal set of three such interferometers can thus measure the position of the center of rotation when $\boldsymbol{\Omega}$ is known from other measurements (e.g. by a set of single loop interferometers). Interferometers with more

than two sequential oppositely directed loops will correspondingly measure second and higher derivatives of the gravitational field.

9. Vibrational immunity

It might seem, at first blush, that the sensitivity of such a system to misalignment from unwanted vibrations will destroy its functionality. Happily, the mechanical rigidity requirements of the neutral atom interferometer described above are much *less* stringent than those of existing operational neutron interferometers. This is largely due to the fact that the diffraction angle, θ, is small. Thus, the waves incident on the detector screen produce a transverse fringe spacing (as noted above) equal to the grating periodicity, which, in turn, is of the order of thousands of angstroms, and not of angstroms as is the case with neutron interferometers. The allowable transverse displacements of a grating is then of this order.

The inherent vibrational immunity of grating interferometers has been long known in their optical counterparts. A rotational displacement of any single grating in the chain has virtually no effect on the interference, but only a second-order displacement of the effective superposition region maximum visibility position. As discussed above, the longitudinal thickness of this region is hundreds of microns, which also then limits the allowable longitudinal displacements of the gratings. The component tolerances compare very favorably with the few angstrom rigidity requirements for neutron interferometers.

Finally, the low velocity of the atoms produces a low-pass filter action for translational and rotational vibrations of the interferometer as a whole. Time response of the system is thus determined by the atomic transit time (0.1 s for the above configuration), and high-frequency vibrations are averaged over automatically.

10. Vacuum requirements

The vacuum requirements are not significantly different than those for neutral atom traps. Both suffer from small angle collisions. Fortunately, background gas atoms will be at a much higher temperature than will be the beam atoms. Nonetheless, in the experiment by Migdall et al. [21] sodium atoms with a maximum velocity of 3.5 m/s were magnetically trapped, and the lifetime of the trapped atoms was limited by the $1\text{–}2 \times 10^{-8}$ Torr vacuum to about 0.8 s. This time is comparable to the transit time for slow atoms in the interferometer described above and thus sets a "ball-park" upper limit to the allowable background pressure in such a system.

11. Neutral atom interferometer with diffraction by crystals

The interferometer configuration discussed above is long and thin. A high aspect ratio has the good features discussed above, namely an inherently high vibrational immunity and an ability to use magnetic field gradients to cancel path curvature at high rotation rates (since all momenta are nearly collinear). It suffers from the fact that for its overall length it encloses comparatively little area. The underlying reason for the long thin configuration is the rather high ratio of the diffraction grating wavelength to the atomic de Broglie wavelength. If one is willing to compromise on some of the above features, then a more compact device can be built by employing a shorter wavelength grating. Classic experiments by Davidson and Germer, by Esterman, Frisch and Stern, and others [19] have demonstrated that neutral atoms show diffraction phenomena in reflection by the cleaved surface of a crystal. The inherently narrow periodicity of the crystal lattice then provides the narrowly spaced grating and allows large deflection angles.

Figure 4 shows configurations for a neutral atom interferometer using diffraction by crystal surfaces. A pair of solenoids generate uniform magnetic fields B1 and B2. Atoms cooled by interaction with the cooling laser beam inside a tapered solenoid are deflected away from the laser beam by passing from B1 to B2 in a manner similar to that of a Rabi deflecting magnet. At the crystal faces, the atomic beam is split by diffraction into different orders and then recombined at the last reflection. The configuration of

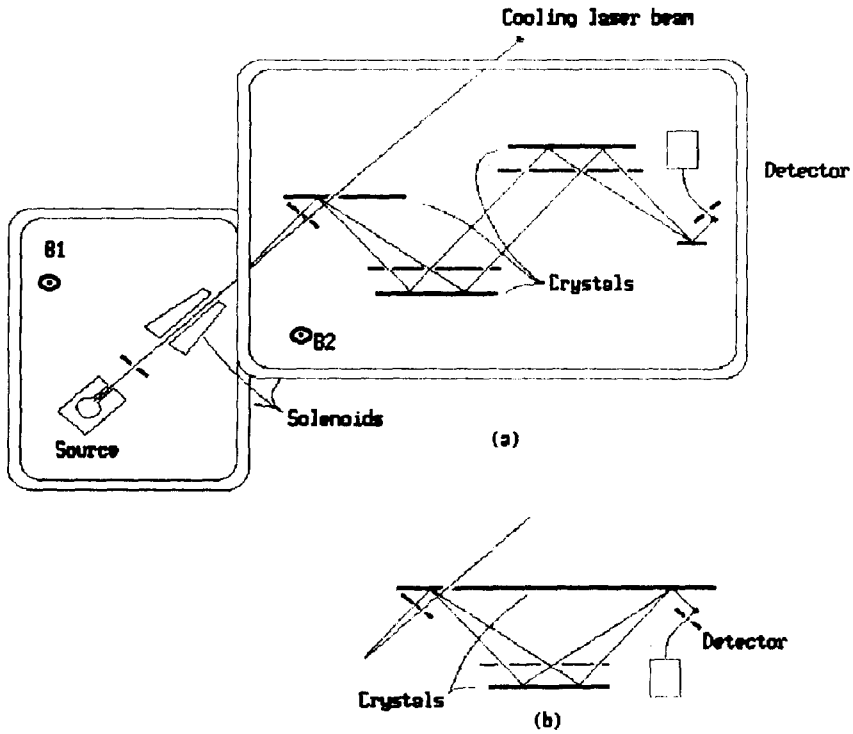

Fig. 4. A neutral atom interferometer using diffractive reflection by crystal surfaces. (a) Interferometer with finite enclosed area. (b) Interferometer with zero area for sensing gravity gradients.

fig. 4a has a finite area and average beam displacement, while that of fig. 4b has zero-enclosed area and thus senses only gravity gradients. A sensitive device can now be made sufficiently compact that mounting it on servo-controlled gimbals is feasible to limit its rotation rate and associated beam sag.

12. Summary

We have shown that matter-wave interferometers employing neutral atoms can be used as inertial sensors with sensitivities that exceed those of conventional mechanical sensors and multiple circuit optical interferometers by many powers of ten. An interferometer in which the propagating beam paths enclose a finite area will sense rotations via the Sagnac effect. One with the paths displaced from each other will sense acceleration plus gravity. The matter-wave energy and mass dependence of the phase shifts that are due to rotation and acceleration are different. Thus a set of interferometers with different orientations, energies and masses can perform simultaneous independent measurements of all components of the rotation rate and acceleration vectors.

An interferometer configuration is proposed. It is formed from a sequence of planar diffraction gratings operating in high order and in either a symmetric or an asymmetric configuration. Useful geometries are generalizations of those employed by Weinberg et al. [14] for light, Marton et al. [15] for electrons, and by Bonse and Hart [16] for neutrons. The configurations feature chromatic focusing, dispersive velocity selection, and excellent immunity to mechanical vibrations. The neutral atom source employs the recently developed laser deceleration and cooling technique for neutral atomic beams. Gratings consist of near-resonant standing-wave laser beams. A variant proposal for a more compact interferometer uses diffractive reflection from crystal surfaces. The interferometer sensitivity is independent of atomic mass (for a given veloci-

ty) and scales inversely with laser wavelength and overall interferometer length squared. Its rotational sensitivity scales inversely with atomic velocity while its accelerational sensitivity scales inversely with atomic velocity squared. Hence slow atoms with a short wavelength resonance transition are preferred.

Additional phase shift may be inserted by introducing controllable spin-parallel magnetic fields that differ between the interferometer paths. Path curvature due to acceleration and rotation can be canceled by magnetic field gradients that produce an effective magnetic levitation of the atoms. A feedback system that maintains an interferometer null can then be employed with its error signal yielding the inertial signals.

Practical scientific applications of the proposed interferometer include measurements of the Lense–Thirring and de Sitter precessions, measurements of the composition-dependent "fifth force", observation of time delays of the gravitational fields of the sun and moon (and thus the speed of gravitational waves), measurement of gravitational gradients, tests of the equivalence principle, and measurements of energy shifts of the total energy of a free atom (such as those due to symmetry breaking effects). Important practical applications of such devices occur in the fields of navigation, geology, surveying and the analysis of structures.

References

[1] A.J. Post, Rev. Mod. Phys. 39 (1967) 475.

[2] S.A. Werner, J.-L. Staudenmann and R. Colella, Phys. Rev. Lett. 42 (1979) 1103.

[3] R. Colella, A.W. Overhauser and S.A. Werner, Phys. Rev. Lett. 34 (1975) 1472.

[4] A.A. Michelson, Astrophys. J. 61 (1925) 137.
A.A. Michelson and H.G. Gale, Astrophys. J. 61 (1925) 140.

[5] S.A. Werner, Physics Today 33 (1980) 24.

[6] A.G. Klein and S.A. Werner, Rep Prog. Phys. 46 (1983) 259.

[7] D.M. Greenberger and A.W. Overhauser, Rev. Mod. Phys. 51 (1979) 43.

[8] The necessary conditions for this criterion to hold are given by R.T. Robiscoe, Am. J. Phys. 39 (1971) 146, and are easily satisfied in such an interferometer configuration.

[9] G. Papini, Nuovo Cimento B 68 (1970) 1.

[10] Two different methods to generate nearly monoenergetic and, more importantly, slow atomic beams have recently been demonstrated. B. Schwartschild, Phys. Today 39 (1986) 17, and D.J. Wineland and W.M. Itano, Phys. Today 40 (1987) 34, discuss such techniques. Presumably, slow, cool molecular beams may be produced by similar means.
J.V. Prodan, W.D. Phillips, and H. Metcalf, Phys. Rev. Lett. 49 (1982) 1149; see also J.V. Prodan et al., Phys. Rev. Lett. 54 (1985) 992, and W.D. Phillips and H. Metcalf, Phys. Rev. Lett. 48 (1982) 596, have described a technique to produce a temporally continuous beam. It involves the use of a tapered magnetic solenoid to continuously Zeeman shift the optical resonance wavelength of the beam as it is slowed and cooled by a counter-propagating laser beam whose wavelength is near that optical resonance.
W. Ertmer, R. Blatt, J.L. Hall and M. Zhu, Phys. Rev. Lett. 54 (1985) 996; see also S. Chu, J.E. Bjorkholm, A. Ashkin and A. Cable, Phys. Rev. Lett. 57 (1986) 314, have described an alternative technique that produces a temporally pulsed beam. It uses a pulsed laser whose wavelength is swept (chirped) during the pulse to maintain resonance as the atoms are being slowed and cooled.

[11] W.W. Chow et al., Rev. Mod. Phys. 57 (1985) 61.
Sanders, W. Schleich, and M.O. Scully, Rev. Mod. Phys. 57 (1985) 61.

[12] Diffraction of neutral atoms by an edge has been observed by J.A. Leavitt and F.A. Bills, Am. J. Phys. 37 (1969) 905. Although these authors claim to have observed single-slit diffraction, there is no evidence presented for an interference of the diffracted rays from opposing edges of the slit.

[13] P.L. Gould, G.A. Ruff and D.E. Pritchard, Phys. Rev. Lett. 56 (1986) 827.

[14] F.J. Weinberg and N.B. Wood, J. Sci. Instrum. 36 (1959) 227.

[15] L. Marton, J.A. Simpson and J.A. Suddeth, Phys. Rev. 90 (1953) 490; Rev. Sci. Instrum. 25 (1954) 1099.
See also J.A. Simpson, Rev. Mod. Phys. 28 (1956) 254; Rev. Sci. Instrum. 25 (1954) 1105;
D. Gabor, Rev. Mod. Phys. 28 (1956) 260.

[16] U. Bonse and M. Hart, Appl. Phys. Lett. 6 (1965) 155.

[17] W.D. Phillips, J.V. Prodan and H.J. Metcalf, J. Opt. Soc. Am. B 2 (1985) 1751.

[18] D.E. Pritchard, in: Electronic and Atomic Collisions, eds. D.C. Lorents et al., (Elsevier, Amsterdam, 1986).

[19] See e.g. N.F. Ramsey, Molecular Beams (Oxford, London, 1969).

[20] B.J. Chang, R. Alferness and E.N. Leith, Appl. Opt. 14 (1975) 1592.

[21] A.L. Migdall, J.V. Prodan, W.D. Phillips, T.H. Bergeman and H.J. Metcalf, Phys. Rev. Lett. 54 (1985) 2596.